

Galaxy-galaxy-galaxy lensing: Third-order correlations between the galaxy and mass distributions in the Universe

Peter Schneider and Peter Watts

Institut f. Astrophysik u. Extr. Forschung, Universität Bonn, Auf dem Hügel 71, D-53121 Bonn, Germany
e-mail: peter@astro.uni-bonn.de, pwatts@astro.uni-bonn.de

Received ; accepted

Abstract. Galaxy-galaxy lensing (GGL) measures the 2-point cross-correlation between galaxies and mass in the Universe. In this work we seek to generalise this effect by considering the *third-order* correlations between galaxies and mass: galaxy-galaxy-galaxy lensing. Third-order correlations in the cosmic shear field have recently been reported in the VIRMOS-DESCART and CTIO surveys. Such data should also be ideal for measuring galaxy-galaxy-galaxy lensing. Indeed, the effects of these higher-order correlations may have already been detected in recent studies of galaxy-galaxy lensing. Higher-order cross-correlation functions contain invaluable information about the relationship between galaxies and their mass environments that GGL studies alone cannot detect.

In this paper we lay out the basic relations for third-order cross correlations and their projections and introduce a new set of scale dependent third-order bias parameters. We define three new observables: two galaxy-shear-shear correlation functions, G_{\pm} , and a galaxy-galaxy-shear correlation, \mathcal{G} . We relate these to the various projected cross-bispectra and give practical estimators for their measurement. We note that the observational signature of these correlators is simply the excess shear-shear correlation measured about foreground galaxies (for G_{\pm}) and the average tangential shear around foreground galaxy pairs (for \mathcal{G}). These quantities are no more than second order in the shear and so should be more easily measurable than the shear 3-point correlation. Finally we derive expressions for the third order aperture mass statistics in terms of both the cross-bispectra and the real-space correlation functions. Such statistics provide a very localized measurement of the bispectra, thus encapsulating essentially all of the available third-order information, while remaining easily obtainable from observations of 3-point cross-correlation functions. In addition we find that utilising aperture statistics has the further benefit that they measure only the *connected* part of the third order correlation.

Key words. cosmology – gravitational lensing – large-scale structure of the Universe – galaxies: evolution – galaxies: statistics

1. Introduction

Gravitational lensing offers the possibility of studying the statistical properties of the mass distribution in the Universe without referring to the relation between the mass and the luminous tracers, like galaxies. The weak lensing effect (see Mellier 1999; Bartelmann & Schneider 2001, hereafter BS01; Refregier 2003; van Waerbeke & Mellier 2003 for recent reviews) of the large-scale structure, called cosmic shear (see, e.g., Blandford et al. 1991; Miralda-Escudé 1991; Kaiser 1992; Jain & Seljak 1997), has been detected by a number of groups (e.g. van Waerbeke et al. 2000, 2001, 2002; Bacon et al. 2000; Kaiser et al. 2000; Wittman et al. 2000; Maoli et al. 2001; Refregier et al. 2002; Hämmerle et al. 2002; Brown et al. 2003; Jarvis et al. 2003). Most of these cosmic shear measurements have concentrated on second-order shear statistics, but quite recently, third-order cosmic shear measurements have been reported as well (Bernardeau et al. 2002; Pen et al. 2003; Jarvis et al. 2004).

Weak lensing can also be used for measuring the relation between mass and galaxies. The measurement of this galaxy-galaxy lensing (GGL) was first attempted by Tyson et al. (1984), and its first detection was published by Brainerd et al. (1996). Since then, quite a number of GGL measurements have been reported, in the HST Medium Deep Survey (Griffiths et al. 1996), the Hubble Deep Field (Dell’Antonio & Tyson 1998; Hudson et al. 1998), and more recently, in the RCS survey by Hoekstra et al. (2001, 2002), the COMBO-17 survey (Kleinheinrich et al. 2004)

and the Sloan Digital Sky Survey (Fischer et al. 2000; McKay et al. 2001; Guzik & Seljak 2002; Sheldon et al. 2004, Seljak et al. 2004). GGL measures the two-point correlation function (2PCF) between galaxy positions and shear.

On small scales, GGL measures the lensing effect of the dark halo in which the luminous galaxy is embedded. It therefore provides a probe of the density profile of galaxy halos which can be compared to the predictions of the CDM model. In particular, the properties of dark matter halos, such as virial mass and concentration, can be studied as a function of galaxy type (early vs. late), environment (e.g., have the halos of galaxies in groups and clusters been stripped by the tidal interactions), and redshift. On scales larger than $\sim 200h^{-1}$ kpc, the GGL signal is no longer dominated by the halo of galaxies, but receives a substantial contribution from the matter in which galaxies are embedded, namely groups and clusters. From this signal, one learns about the environments of galaxies. For example, the density-morphology relation can be traced back directly to the underlying mass density, instead to the galaxy number density.

Schneider (1998) pointed out that the correlation between galaxy positions and shear provides a direct measure of the bias factor of galaxies; in particular, the scale dependence of the bias factor can be probed directly (van Waerbeke 1998). Indeed, on scales $\gtrsim 2h^{-1}$ Mpc, GGL measures a combination of the galaxy-mass correlation coefficient r and the bias factor b . These two functions can be obtained individually when the GGL signal is combined with the cosmic shear signal, as shown by Hoekstra et al. (2002). In fact, Hoekstra et al. (2002) have measured r and b as a function of scale. Future measurements of these quantities as a function of scale, redshift and galaxy type, using the upcoming wide-field imaging surveys, will provide invaluable input for the interpretation of galaxy redshift samples. In addition, b and r are functions which depend on the formation and evolution of galaxies; they can therefore be used as constraints for those models.

As already mentioned, a non-vanishing cosmic shear three-point correlation function (3PCF) has been detected, and future surveys will measure it with great precision. These surveys will certainly also measure higher-order correlations between galaxies and matter, generalizing the GGL measurements. Although the detailed physical interpretation of such higher-order cross correlations remains to be investigated, it is obvious that they contain valuable information concerning the relationship between galaxies and their mass environments *beyond* that which is measurable in GGL. In the language of the halo occupation distribution (Berlind & Weinberg 2002), one can think of these higher-order functions as probing the moments of an occupation probability $P(N|M)$ that a halo of virial mass M contains N galaxies of a particular type. Such information is of crucial importance since it places powerful constraints upon models of galaxy formation.

We save the detailed interpretation of higher-order cross correlations for a forthcoming paper, where we explore such themes in the context of the halo model. In this work we lay out the basic relations for the third-order galaxy-mass correlations. After introducing the projected mass and galaxy number densities in Sect. 2, we define the third-order bias factor and two third-order correlation coefficients in Sect. 3. The relation between the projected bispectra and the three-dimensional bispectra is given in Sect. 4. Practical estimators for the galaxy-galaxy-shear and the galaxy-shear-shear correlation functions are provided in Sect. 5. We will argue that these third-order galaxy-mass correlations have already been measured and published. In Sect. 6, the relation between the correlation functions and the cross-bispectra are derived, and a consistency relation for the two galaxy-shear-shear 3PCFs is obtained that should be satisfied provided the shear is a pure E-mode field. In Sect. 7 we define aperture measures of the projected matter and galaxy densities and consider their third-order statistics; in particular, on the one hand they are related to the projected bispectra, on the other hand, they can be directly calculated from the respective correlation functions. We discuss our results in Sect. 8.

Ménard et al. (2003) have considered a different approach to measure third-order correlations between the mass and the galaxy distribution, employing the magnification bias of background galaxies. Generalizing an effect that has been observed at the two-point statistical level, where correlations between high-redshift QSOs and low redshift galaxies are observed and which are interpreted as being due to the magnification caused by the large-scale matter distribution of which the foreground galaxies are biased tracers (see Dolag & Bartelmann, 1997; Bartelmann & Schneider 2001, and references therein), Ménard et al. (2003) considered the excess of distant QSOs around pairs of foreground galaxies. For linear deterministic bias of the galaxy distribution, the ratio of this third-order statistics and the square of the QSO-galaxy correlation function becomes essentially independent of the bias, as well as of the shape and amplitude of the power spectrum of density fluctuations. This result is very similar to the corresponding ratio of third-order cosmic shear statistics and the square of the shear dispersion (Bernardeau et al. 1997; Schneider et al. 1998; van Waerbeke et al. 1999).

2. Projection of density and galaxies

The gravitational lensing effect of the inhomogeneous matter distribution in the Universe is described in terms of an equivalent surface mass density $\kappa(\boldsymbol{\theta})$, which is obtained by projecting the three-dimensional density contrast, δ , of the

matter along the line-of-sight (see BS01, and references therein). If we consider sources at comoving distance w , this surface mass density is given by

$$\kappa(\boldsymbol{\theta}, w) = \frac{3H_0^2\Omega_m}{2c^2} \int_0^w dw' \frac{f_K(w')f_K(w-w')}{f_K(w)} \frac{\delta(f_K(w')\boldsymbol{\theta}, w')}{a(w')}, \quad (1)$$

where $f_K(w)$ is the comoving angular-diameter distance corresponding to comoving distance w , $f_K(w) = w$ for flat Universes, $\delta = \Delta\rho/\bar{\rho}$ is the relative density contrast of matter, H_0 is the Hubble constant, c the velocity of light, $a(w) = 1/(1+z)$ is the cosmic scale factor, normalized to unity today, and Ω_m is the density parameter in matter. For a redshift distribution of ('background') sources with probability density $p_z(z) dz = p_w(w) dw$, the effective surface mass density becomes

$$\kappa(\boldsymbol{\theta}) = \int dw p_w(w) \kappa(\boldsymbol{\theta}, w) = \frac{3H_0^2\Omega_m}{2c^2} \int_0^{w_h} dw g(w) f_K(w) \frac{\delta(f_K(w)\boldsymbol{\theta}, w)}{a(w)}, \quad (2)$$

with

$$g(w) = \int_w^{w_h} dw' p_w(w') \frac{f_K(w' - w)}{f_K(w')}, \quad (3)$$

which is the source-redshift weighted lens efficiency factor D_{ds}/D_s for a density fluctuation at distance w . The quantity w_h is the comoving horizon distance, obtained from $w(a)$ by letting $a \rightarrow 0$. The shear, i.e. the projected tidal gravitational field which can be measured as the expectation value of image ellipticities of the galaxy population, is obtained from the projected surface mass density κ in the usual way: one defines the deflection potential $\psi(\boldsymbol{\theta})$ which satisfies the two-dimensional Poisson equation $\nabla^2\psi = 2\kappa$, in terms of which the Cartesian components of the shear read $\gamma_1 = (\psi_{,11} - \psi_{,22})/2$, $\gamma_2 = \psi_{,12}$, where indices separated by a comma denote partial derivatives.

In analogy to the matter density contrast δ , we define the number density contrast $\delta_g(\boldsymbol{x}, w)$ of galaxies as

$$\delta_g(\boldsymbol{x}, w) := \frac{n(\boldsymbol{x}, w) - \bar{n}(w)}{\bar{n}(w)}, \quad (4)$$

where $n(\boldsymbol{x}, w)$ is the number density of galaxies at comoving position \boldsymbol{x} and comoving distance w (the latter providing a parameterization of cosmic time), and $\bar{n}(w)$ is the mean number density of galaxies at that epoch. Since the galaxy distribution is discrete, the true number density is simply a sum of delta-functions. What is meant by n is that the probability of finding a galaxy in the volume dV situated at position \boldsymbol{x} is $n(\boldsymbol{x}) dV$. We consider now a population of ('foreground') galaxies with spatial number density $n(\boldsymbol{x}, w)$. The number density of these galaxies on the sky at $\boldsymbol{\theta}$ is then $N(\boldsymbol{\theta}) = \int dw \nu(w) n(f_K(w)\boldsymbol{\theta}, w)$, where $\nu(w)$ is the redshift-dependent selection function, describing what fraction of the galaxies at comoving distance w is included in the sample. The selection function $\nu(w)$ can differ between different types of foreground galaxies and thus depends on the sample selection. The mean number density of these galaxies on the sky is $\bar{N} = \int dw \nu(w) \bar{n}(w)$; the redshift distribution of these galaxies, or more precisely, their distribution in comoving distance therefore is $p_f(w) = \nu(w) \bar{n}(w) / \bar{N}$, thus relating the selection function $\nu(w)$ to the redshift distribution. Using the definition (4), one then finds for the number density of galaxies $N(\boldsymbol{\theta})$ on the sky and their fractional number density contrast $\kappa_g(\boldsymbol{\theta})$,

$$N(\boldsymbol{\theta}) = \bar{N} \left[1 + \int dw p_f(w) \delta_g(f_K(w)\boldsymbol{\theta}, w) \right]; \quad \kappa_g(\boldsymbol{\theta}) := [N(\boldsymbol{\theta}) - \bar{N}] / \bar{N} = \int dw p_f(w) \delta_g(f_K(w)\boldsymbol{\theta}, w). \quad (5)$$

3. Definition of bias and correlation coefficients

3.1. Second-order statistics

In its simplest form, the relation between the density contrast δ and the fractional number density contrast δ_g of galaxies is described by the bias factor b , in the form $\delta_g = b\delta$. This picture of linear deterministic biasing is most likely too simple a description for the galaxy distribution, at least on small spatial scales where the density field is non-linear. Instead, one defines the bias parameter in terms of the power spectra of the galaxy and matter distribution. Let $\hat{\delta}(\mathbf{k})$ and $\hat{\delta}_g(\mathbf{k})$ be the Fourier transforms of the density and galaxy contrast, respectively; their power spectra $P_{\delta\delta}$ and P_{gg} are defined by the correlators

$$\left\langle \hat{\delta}(\mathbf{k}, w) \hat{\delta}^*(\mathbf{k}', w) \right\rangle = (2\pi)^3 \delta_D(\mathbf{k} - \mathbf{k}') P_{\delta\delta}(|\mathbf{k}|, w); \quad \left\langle \hat{\delta}_g(\mathbf{k}, w) \hat{\delta}_g^*(\mathbf{k}', w) \right\rangle = (2\pi)^3 \delta_D(\mathbf{k} - \mathbf{k}') P_{gg}(|\mathbf{k}|, w), \quad (6)$$

where δ_D denotes Dirac's delta-'function', and we have allowed for an evolution of the power spectra with redshift or comoving distance w . The occurrence of the delta function is due to the assumed statistical homogeneity of the

random matter and galaxy fields, and the fact that the power spectra depends only on the modulus of \mathbf{k} is due to their statistical isotropy. The bias parameter $b(k, w)$ is defined by the ratio of these two power spectra,

$$P_{\text{gg}}(k, w) = b^2(k, w) P_{\delta\delta}(k, w), \quad (7)$$

which agrees with the previous definition in the case of linear deterministic biasing, but is far more general. In particular, we allow for a scale- and redshift dependence of b . Next, we define the cross-power spectrum $P_{\delta\text{g}}(k, w)$ through

$$\langle \hat{\delta}(\mathbf{k}, w) \hat{\delta}_{\text{g}}^*(\mathbf{k}', w) \rangle = (2\pi)^3 \delta_{\text{D}}(\mathbf{k} - \mathbf{k}') P_{\delta\text{g}}(|\mathbf{k}|, w); \quad (8)$$

The cross-power spectrum is related to the power spectrum of the matter density by

$$P_{\delta\text{g}}(k, w) = b(k, w) r(k, w) P_{\delta\delta}(k, w), \quad (9)$$

where we have defined the galaxy-mass correlation coefficient $r(k, w)$, which can also depend on scale and redshift. In the case of linear deterministic biasing, $r \equiv 1$.

3.2. Third-order statistics

We now generalize the foregoing definitions to third-order statistics. The bispectra of the matter and galaxy distributions are defined through the triple correlators

$$\begin{aligned} \langle \hat{\delta}(\mathbf{k}_1) \hat{\delta}(\mathbf{k}_2) \hat{\delta}(\mathbf{k}_3) \rangle &= (2\pi)^3 \delta_{\text{D}}(\mathbf{k}_1 + \mathbf{k}_2 + \mathbf{k}_3) B_{\delta\delta\delta}(\mathbf{k}_1, \mathbf{k}_2, \mathbf{k}_3; w), \\ \langle \hat{\delta}_{\text{g}}(\mathbf{k}_1) \hat{\delta}_{\text{g}}(\mathbf{k}_2) \hat{\delta}_{\text{g}}(\mathbf{k}_3) \rangle &= (2\pi)^3 \delta_{\text{D}}(\mathbf{k}_1 + \mathbf{k}_2 + \mathbf{k}_3) B_{\text{ggg}}(\mathbf{k}_1, \mathbf{k}_2, \mathbf{k}_3; w), \end{aligned} \quad (10)$$

where the delta function ensures that these triple correlators vanish unless the three \mathbf{k} -vectors form a closed triangle – this property again follows from the statistical homogeneity of the density fields. Furthermore, statistical isotropy causes the bispectrum to depend only on the length of two of its \mathbf{k} -vectors and the angle they enclose. Finally, parity invariance of the density fields requires that the bispectra are even functions of this angle. In a similar spirit to Eq. (8) we can define the cross-bispectra

$$\begin{aligned} \langle \hat{\delta}(\mathbf{k}_1) \hat{\delta}(\mathbf{k}_2) \hat{\delta}_{\text{g}}(\mathbf{k}_3) \rangle &= (2\pi)^3 \delta_{\text{D}}(\mathbf{k}_1 + \mathbf{k}_2 + \mathbf{k}_3) B_{\delta\delta\text{g}}(\mathbf{k}_1, \mathbf{k}_2; \mathbf{k}_3; w), \\ \langle \hat{\delta}_{\text{g}}(\mathbf{k}_1) \hat{\delta}_{\text{g}}(\mathbf{k}_2) \hat{\delta}(\mathbf{k}_3) \rangle &= (2\pi)^3 \delta_{\text{D}}(\mathbf{k}_1 + \mathbf{k}_2 + \mathbf{k}_3) B_{\text{gg}\delta}(\mathbf{k}_1, \mathbf{k}_2; \mathbf{k}_3; w). \end{aligned} \quad (11)$$

where we have introduced the notation $(\mathbf{k}_1, \mathbf{k}_2; \mathbf{k}_3)$ to indicate the symmetry with respect to interchanging the first two arguments, meaning, e.g., that $B_{\text{gg}\delta}(\mathbf{k}_1, \mathbf{k}_2; -\mathbf{k}_1 - \mathbf{k}_2) = B_{\text{gg}\delta}(\mathbf{k}_2, \mathbf{k}_1; -\mathbf{k}_1 - \mathbf{k}_2)$.

In the case of linear deterministic biasing, the various bispectra would be related through simple relations, e.g., $B_{\text{ggg}} = b^2 B_{\delta\delta\delta}$. However, in the more general (and realistic) case, these relations are more complex. We define the third-order bias parameter b_3 and the two galaxy-mass correlation coefficients r_1 and r_2 through the relations

$$B_{\text{ggg}}(\mathbf{k}_1, \mathbf{k}_2, \mathbf{k}_3; w) = b_3^3(\mathbf{k}_1, \mathbf{k}_2, \mathbf{k}_3; w) B_{\delta\delta\delta}(\mathbf{k}_1, \mathbf{k}_2, \mathbf{k}_3; w), \quad (12)$$

$$B_{\text{gg}\delta}(\mathbf{k}_1, \mathbf{k}_2; \mathbf{k}_3; w) = b_3^2(\mathbf{k}_1, \mathbf{k}_2, \mathbf{k}_3; w) r_2(\mathbf{k}_1, \mathbf{k}_2; \mathbf{k}_3; w) B_{\delta\delta\delta}(\mathbf{k}_1, \mathbf{k}_2, \mathbf{k}_3; w), \quad (12)$$

$$B_{\delta\delta\text{g}}(\mathbf{k}_1, \mathbf{k}_2; \mathbf{k}_3; w) = b_3(\mathbf{k}_1, \mathbf{k}_2, \mathbf{k}_3; w) r_1(\mathbf{k}_1, \mathbf{k}_2; \mathbf{k}_3; w) B_{\delta\delta\delta}(\mathbf{k}_1, \mathbf{k}_2, \mathbf{k}_3; w). \quad (13)$$

The bias and correlation coefficients satisfy the same symmetries as those of the bispectra. In the case of linear deterministic biasing, $b_3 = b$ and $r_1 = 1 = r_2$. These higher-order biasing and correlation parameters depend on the formation and evolution of galaxies and their relation to the underlying density field; in general, they encapsulate information concerning the non-Gaussian nature of the bias. As we show in the next section, the correlation of lensing shear with the positions of galaxies on the sky provides a direct means for measuring (integrals of) these higher-order functions.

4. Projected power- and bispectra

The lensing effect and the position of galaxies on the sky are both described by projections of the density field δ and the galaxy field δ_{g} along the line-of-sight, as shown in Sect. 2. The projected fields share the properties of the three-dimensional distributions as being homogeneous and isotropic random fields; hence, their second- and third-order properties can as well be described by power and bispectra. The relation between the power spectra of projected

quantities to that of the three-dimensional distribution is given by Limber's equation in Fourier space, as has been derived by Kaiser (1992): Let

$$\kappa_i(\boldsymbol{\theta}) = \int dw q_i(w) \delta_i(f_K(w)\boldsymbol{\theta}, w) \quad (14)$$

be projections of the 3-D fields δ_i , where the $q_i(w)$ are weight functions depending on the comoving distance. Provided these weight functions do not vary appreciably over comoving scales on which the power spectrum is significantly different from zero, the (cross) power spectrum reads

$$P_{12}(\ell) = \int dw \frac{q_1(w) q_2(w)}{f_K^2(w)} P_\delta\left(\frac{\ell}{f_K(w)}, w\right). \quad (15)$$

Hence, the 2-D power at angular scale $2\pi/\ell$ is obtained from the 3-D power at length scale $f_K(w) (2\pi/\ell)$, integrated over w . For the power spectra of the projected mass density κ and the galaxies κ_g , and the cross-power of these two quantities, we therefore find, by comparing Eqs. (14) and (15) with (2) and (5),

$$\begin{aligned} P_{\kappa\kappa}(\ell) &= \frac{9H_0^4\Omega_m^2}{4c^4} \int_0^{w_h} dw \frac{g^2(w)}{a^2(w)} P_{\delta\delta}(k; w); & P_{\text{gg}}(\ell) &= \int dw \frac{p_f^2(w)}{f_K^2(w)} b^2(k; w) P_{\delta\delta}(k; w); \\ P_{\kappa_g}(\ell) &= \frac{3H_0^2\Omega_m}{2c^2} \int dw \frac{g(w) p_f(w)}{f_K(w) a(w)} b(k; w) r(k; w) P_{\delta\delta}(k; w), \end{aligned} \quad (16)$$

where $\mathbf{k} = \ell/f_K(w)$ and where we have used the definition of the bias and galaxy-mass parameters given in Sect. 3.1. The quantity $P_{\kappa\kappa}(\ell)$ is the power spectrum probed by second-order cosmic shear measurements whereas $P_{\text{gg}}(\ell)$ is the power spectrum of the galaxy distribution [with the selection function specified by $p_f(w)$] on the sky, i.e., the Fourier transform of the angular 2PCF of galaxies. The cross-power $P_{\kappa_g}(\ell)$ is the quantity that is measured in galaxy-galaxy lensing observations; see Hoekstra et al. (2002).

The bispectrum of the projected quantities (14) is defined in terms of the triple correlator

$$\langle \hat{\kappa}_1(\boldsymbol{\ell}_1) \hat{\kappa}_2(\boldsymbol{\ell}_2) \hat{\kappa}_3(\boldsymbol{\ell}_3) \rangle = (2\pi)^2 \delta_D(\boldsymbol{\ell}_1 + \boldsymbol{\ell}_2 + \boldsymbol{\ell}_3) b_{123}(\boldsymbol{\ell}_1, \boldsymbol{\ell}_2, \boldsymbol{\ell}_3), \quad (17)$$

where the relation between the bispectrum of the projected quantities κ and the 3-D bispectrum is given by

$$b_{123}(\boldsymbol{\ell}_1, \boldsymbol{\ell}_2, \boldsymbol{\ell}_3) = \int dw \frac{q_1(w) q_2(w) q_3(w)}{f_K^4(w)} B_{123}\left(\frac{\boldsymbol{\ell}_1}{f_K(w)}, \frac{\boldsymbol{\ell}_2}{f_K(w)}, \frac{\boldsymbol{\ell}_3}{f_K(w)}; w\right), \quad (18)$$

which is valid under the same conditions required for the validity of (15), i.e., the weight functions $q_i(w)$ should not vary appreciably over scales on which the bispectrum is significantly non-zero. Inserting into this relation the weight functions q appropriate for the surface mass density κ and the projected number density κ_g , one obtains the bispectra

$$b_{\kappa\kappa\kappa}(\boldsymbol{\ell}_1, \boldsymbol{\ell}_2, \boldsymbol{\ell}_3) = \frac{27H_0^6\Omega_m^3}{8c^6} \int dw \frac{g^3(w)}{f_K(w) a^3(w)} B_{\delta\delta\delta}(\mathbf{k}_1, \mathbf{k}_2, \mathbf{k}_3; w), \quad (19)$$

$$b_{\kappa\kappa_g}(\boldsymbol{\ell}_1, \boldsymbol{\ell}_2; \boldsymbol{\ell}_3) = \frac{9H_0^4\Omega_m^2}{4c^4} \int dw \frac{g^2(w) p_f(w)}{f_K^2(w) a^2(w)} [b_3 r_1 B_{\delta\delta\delta}](\mathbf{k}_1, \mathbf{k}_2; \mathbf{k}_3; w) =: [\bar{b}_3 \bar{r}_1 b_{\kappa\kappa\kappa}](\boldsymbol{\ell}_1, \boldsymbol{\ell}_2; \boldsymbol{\ell}_3), \quad (20)$$

$$b_{\text{gg}\kappa}(\boldsymbol{\ell}_1, \boldsymbol{\ell}_2; \boldsymbol{\ell}_3) = \frac{3H_0^2\Omega_m}{2c^2} \int dw \frac{g(w) p_f^2(w)}{f_K^3(w) a(w)} [b_3^2 r_2 B_{\delta\delta\delta}](\mathbf{k}_1, \mathbf{k}_2; \mathbf{k}_3; w) =: [\bar{b}_3^2 \bar{r}_2 b_{\kappa\kappa\kappa}](\boldsymbol{\ell}_1, \boldsymbol{\ell}_2; \boldsymbol{\ell}_3) \quad (21)$$

$$b_{\text{ggg}}(\boldsymbol{\ell}_1, \boldsymbol{\ell}_2, \boldsymbol{\ell}_3) = \int dw \frac{p_f^3(w)}{f_K^4(w)} [b_3^3 B_{\delta\delta\delta}](\mathbf{k}_1, \mathbf{k}_2, \mathbf{k}_3; w) =: [\bar{b}_3^3 b_{\kappa\kappa\kappa}](\boldsymbol{\ell}_1, \boldsymbol{\ell}_2, \boldsymbol{\ell}_3), \quad (22)$$

where again the vectors $\mathbf{k}_i = \boldsymbol{\ell}_i/f_K(w)$, and we have defined the projected bias factor \bar{b}_3 and correlation coefficients \bar{r}_1 , \bar{r}_2 , which depend, in addition to the angular wave vectors $\boldsymbol{\ell}_i$, on the redshift distribution of foreground and background galaxies. The correlations are strongest if the redshift distribution of the foreground galaxies matches the most efficient lensing redshift for a given source redshift distribution – see Hoekstra et al. (2002) for a similar discussion in the context of second-order galaxy-mass correlations.

5. Estimators

The basic observables for the second-order statistics obtained from observational data are the 2PCFs. Hence, the angular 2PCF of galaxies $\omega(\boldsymbol{\theta}) = \langle \kappa_g(\boldsymbol{\phi}) \kappa_g(\boldsymbol{\phi} + \boldsymbol{\theta}) \rangle$ is the Fourier transform of $P_{\text{gg}}(\ell)$. The second-order statistics of the projected matter density are probed by the shear 2PCFs $\xi_\pm(\boldsymbol{\theta})$. They are defined in the following way: let $\gamma_c = \gamma_1 + i\gamma_2$ denote the complex shear in Cartesian coordinates. Given a direction φ , we define the rotated shear

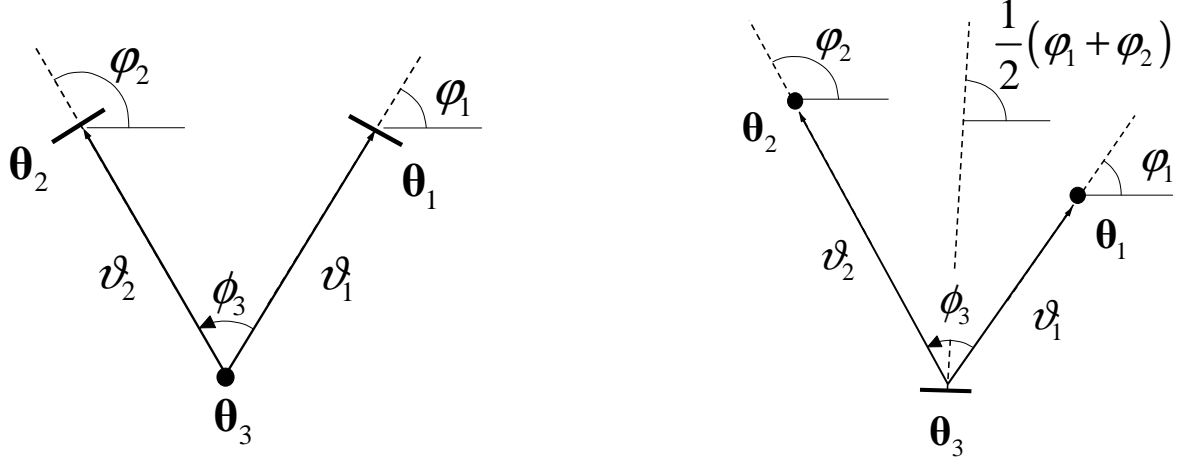


Fig. 1. Geometry of the galaxy-shear-shear correlation, $G_{\pm}(\vartheta_1, \vartheta_2, \phi_3)$ (left panel), and the galaxy-galaxy-shear correlation, $\mathcal{G}(\vartheta_1, \vartheta_2, \phi_3)$ (right panel). Note that the sign of the angle $\phi_3 = \varphi_2 - \varphi_1$ is important.

$\gamma(\boldsymbol{\theta}; \varphi) = -e^{-2i\varphi} \gamma_c(\boldsymbol{\theta})$. This definition implies that $\gamma(\boldsymbol{\theta}; \varphi_1) = \gamma(\boldsymbol{\theta}; \varphi_2) e^{2i(\varphi_2 - \varphi_1)}$. The real and imaginary part of $\gamma(\boldsymbol{\theta}; \varphi)$ are the tangential and cross component of the shear relative to the direction φ (see, e.g., Crittenden et al. 2002; Schneider et al. 2002). Hence the shear 2PCFs are written as

$$\xi_+(\theta) = \langle \gamma(\boldsymbol{\phi}; \varphi) \gamma^*(\boldsymbol{\phi} + \boldsymbol{\theta}; \varphi) \rangle ; \quad \xi_-(\theta) = \langle \gamma(\boldsymbol{\phi}; \varphi) \gamma(\boldsymbol{\phi} + \boldsymbol{\theta}; \varphi) \rangle , \quad (23)$$

where the average is over all pairs of points with angular separation θ , and φ is the polar angle of their separation vector $\boldsymbol{\theta}$. The imaginary parts of ξ_{\pm} vanish due to parity invariance (e.g., Schneider 2003). For a set of observed galaxies, the shear in (23) is replaced by the image ellipticities, which are an unbiased estimator of the shear (we neglect here the difference between shear and reduced shear; see BS01). The shear 2PCFs are related in a simple way to the power spectrum $P_{\kappa\kappa}(\ell)$ – see Kaiser (1992).

The cross-power is probed by the galaxy-galaxy lensing signal, which correlates the tangential component of the shear at the location of a background galaxy with the position of a foreground galaxy. We define this correlation function as

$$\langle \gamma_t \rangle(\theta) = \langle \kappa_g(\boldsymbol{\phi}) \gamma(\boldsymbol{\phi} + \boldsymbol{\theta}; \varphi) \rangle \quad (24)$$

(e.g., Hoekstra et al. 2002), where φ is, as before, the polar angle of the connection vector $\boldsymbol{\theta}$, and the imaginary part of (24) vanishes due to parity invariance. A practical estimator for $\langle \gamma_t \rangle$ is obtained by averaging the tangential shear component of the background galaxies in all foreground-background pairs with separation θ .

Similarly, the third-order statistics are best probed from observing the 3PCFs. The angular 3PCF of galaxies is one of the standard ways to characterize the non-Gaussian properties of the galaxy distribution on the sky, and standard methods for estimating it are known (see, e.g., Peebles 1980). The bispectrum $b_{\kappa\kappa\kappa}$ is probed by the shear 3PCF, as defined in Schneider & Lombardi (2003; see also Takada & Jain 2003a; Zaldarriaga & Scoccimarro 2003), and its relation to the bispectrum has been derived in Schneider et al. (2004). We next derive expressions for the correlation functions related to the cross-bispectra.

5.1. Galaxy-shear-shear correlation

Consider a triplet of points, where two background galaxies are located at $\boldsymbol{\theta}_1$ and $\boldsymbol{\theta}_2$, and a foreground galaxy is located at $\boldsymbol{\theta}_3$ (see Fig. 1, left). We define the following galaxy-shear-shear 3PCFs

$$G_+(\boldsymbol{\vartheta}_1, \boldsymbol{\vartheta}_2) = G_+(\vartheta_1, \vartheta_2, \phi_3) = \langle \gamma(\boldsymbol{\theta}_1; \varphi_1) \gamma^*(\boldsymbol{\theta}_2; \varphi_2) \kappa_g(\boldsymbol{\theta}_3) \rangle , \quad (25)$$

$$G_-(\boldsymbol{\vartheta}_1, \boldsymbol{\vartheta}_2) = G_-(\vartheta_1, \vartheta_2, \phi_3) = \langle \gamma(\boldsymbol{\theta}_1; \varphi_1) \gamma(\boldsymbol{\theta}_2; \varphi_2) \kappa_g(\boldsymbol{\theta}_3) \rangle , \quad (26)$$

where the separation vectors between the background galaxies and the foreground galaxy are $\boldsymbol{\vartheta}_i = \boldsymbol{\theta}_i - \boldsymbol{\theta}_3$ for $i = 1, 2$, and φ_i is the polar direction of the separation vector $\boldsymbol{\vartheta}_i$. These correlation functions depend on the moduli

of the separation vectors $\boldsymbol{\vartheta}_i$ and the angle ϕ_3 enclosed by them. In order to find a practical estimator for these cross-correlations, it is useful to consider the modified correlators

$$\tilde{G}_+(\vartheta_1, \vartheta_2, \phi_3) = \frac{1}{N} \langle \gamma(\boldsymbol{\theta}_1; \varphi_1) \gamma^*(\boldsymbol{\theta}_2; \varphi_2) N(\boldsymbol{\theta}_3) \rangle, \quad \tilde{G}_-(\vartheta_1, \vartheta_2, \phi_3) = \frac{1}{N} \langle \gamma(\boldsymbol{\theta}_1; \varphi_1) \gamma(\boldsymbol{\theta}_2; \varphi_2) N(\boldsymbol{\theta}_3) \rangle. \quad (27)$$

Using $N/\bar{N} = 1 + \kappa_g$, these modified correlators become

$$\tilde{G}_+(\vartheta_1, \vartheta_2, \phi_3) = G_+(\vartheta_1, \vartheta_2, \phi_3) + \langle \gamma(\boldsymbol{\theta}_1; \varphi_1) \gamma^*(\boldsymbol{\theta}_2; \varphi_2) \rangle = G_+(\vartheta_1, \vartheta_2, \phi_3) + \xi_+(\Delta\theta) e^{2i\phi_3}, \quad (28)$$

$$\tilde{G}_-(\vartheta_1, \vartheta_2, \phi_3) = G_-(\vartheta_1, \vartheta_2, \phi_3) + \langle \gamma(\boldsymbol{\theta}_1; \varphi_1) \gamma(\boldsymbol{\theta}_2; \varphi_2) \rangle = G_-(\vartheta_1, \vartheta_2, \phi_3) + \xi_-(\Delta\theta) \frac{(\vartheta_2 e^{i\phi_3/2} - \vartheta_1 e^{-i\phi_3/2})^4}{(\Delta\theta)^4}, \quad (29)$$

where $\Delta\theta = |\boldsymbol{\vartheta}_2 - \boldsymbol{\vartheta}_1|$ is the separation between the two background galaxies. The phase factors with which the shear 2PCFs are multiplied are obtained by rotating the shears from the direction pointing towards the foreground galaxy to that of the separation vector of the two background galaxies. If the polar angle of the latter is denoted by φ_Δ , then $\gamma(\boldsymbol{\theta}_i; \varphi_i) = \gamma(\boldsymbol{\theta}_i; \varphi_\Delta) e^{2i(\varphi_\Delta - \varphi_i)}$, from which the expressions for the phase factors follow. Hence, the modified galaxy-shear-shear correlators are given by the sum of the (reduced) galaxy-shear-shear correlators G_\pm (which is proportional to the cross-bispectrum $b_{\kappa\kappa g}$) plus the 2PCF of cosmic shear (23), modified by a phase factor that accounts for the fact that the projection directions of the shear are φ_i , and thus do not correspond to the separation vector between the background galaxy pair.

We can obtain practical estimators for these cross 3PCFs, as follows: first, one defines bins in $(\vartheta_1, \vartheta_2, \phi_3)$ -space. Then, for each triplet of two background galaxies and one foreground galaxy whose separation falls inside a given bin, one adds the product of shears, so that

$$\tilde{G}_+(\vartheta_1, \vartheta_2, \phi_3) = \frac{1}{N_{\text{triplet}}} \sum_{\text{triplet}} \gamma(\boldsymbol{\theta}_1; \varphi_1) \gamma^*(\boldsymbol{\theta}_2; \varphi_2); \quad \tilde{G}_-(\vartheta_1, \vartheta_2, \phi_3) = \frac{1}{N_{\text{triplet}}} \sum_{\text{triplet}} \gamma(\boldsymbol{\theta}_1; \varphi_1) \gamma(\boldsymbol{\theta}_2; \varphi_2). \quad (30)$$

These estimators can be easily calculated from the catalog of galaxy positions and ellipticities, e.g., using the method of Jarvis et al. (2004) for finding triplets. From the estimator above, the contribution of the shear 2PCF according to (29) has to be subtracted in order to obtain the reduced galaxy-shear-shear 3PCF G_\pm . Note that observationally the galaxy-shear-shear correlation is simply the excess of the shear 2PCF measured around foreground galaxies.

5.2. Galaxy-galaxy-shear correlation

Next we consider the 3PCF between the shear of one background galaxy and the positions of two foreground galaxies. Let the former be at position $\boldsymbol{\theta}_3$, the latter at positions $\boldsymbol{\theta}_1$ and $\boldsymbol{\theta}_2$, then we define the reduced galaxy-galaxy-shear correlation function as

$$\mathcal{G}(\boldsymbol{\vartheta}_1, \boldsymbol{\vartheta}_2) = \mathcal{G}(\vartheta_1, \vartheta_2, \phi_3) = \left\langle \kappa_g(\boldsymbol{\theta}_1) \kappa_g(\boldsymbol{\theta}_2) \gamma \left(\boldsymbol{\theta}_3; \frac{\varphi_1 + \varphi_2}{2} \right) \right\rangle, \quad (31)$$

where, as before, $\boldsymbol{\theta}_i = \boldsymbol{\theta}_3 + \boldsymbol{\vartheta}_i$, and φ_i is the polar angle of the vector $\boldsymbol{\vartheta}_i$, for $i = 1, 2$ (see Fig. 1, right). The shear in (31) is projected along the line which bisects the angle between the two foreground galaxies, as measured from the background galaxy. As before, for obtaining a practical estimator it is useful to first define a modified 3PCF,

$$\tilde{\mathcal{G}}(\boldsymbol{\vartheta}_1, \boldsymbol{\vartheta}_2) = \tilde{\mathcal{G}}(\vartheta_1, \vartheta_2, \phi_3) = \frac{1}{N^2} \left\langle N(\boldsymbol{\theta}_1) N(\boldsymbol{\theta}_2) \gamma \left(\boldsymbol{\theta}_3; \frac{\varphi_1 + \varphi_2}{2} \right) \right\rangle. \quad (32)$$

Using again $N/\bar{N} = 1 + \kappa_g$, and applying the transformation law for rotating shears, this can be written as

$$\tilde{\mathcal{G}}(\boldsymbol{\vartheta}_1, \boldsymbol{\vartheta}_2) = \tilde{\mathcal{G}}(\vartheta_1, \vartheta_2, \phi_3) = \mathcal{G}(\vartheta_1, \vartheta_2, \phi_3) + \langle \gamma_t \rangle (\vartheta_1) e^{-i\phi_3} + \langle \gamma_t \rangle (\vartheta_2) e^{i\phi_3}, \quad (33)$$

where the last two terms are the two-point galaxy-shear correlation functions (24), obtained from rotating the shear in the direction of the two foreground galaxies. Hence, the correlator $\tilde{\mathcal{G}}$ is the sum of the reduced galaxy-galaxy-shear correlation function plus the two GGL contributions which would be present even for the case of purely Gaussian density fields. A practical estimator for $\tilde{\mathcal{G}}$ is obtained by finding triplets of galaxies that fall in a given bin, and then summing over the shears of the background galaxies,

$$\tilde{\mathcal{G}} = \frac{1}{N_{\text{triplet}}} \sum_{\text{triplet}} \gamma \left(\boldsymbol{\theta}_i; \frac{\varphi_1 + \varphi_2}{2} \right). \quad (34)$$

The signature of the galaxy-galaxy-shear correlation is therefore just the excess shear measured about pairs of foreground galaxies.

Note that integral measures of these three-point cross-correlation functions have probably been measured already. McKay et al. (2002) have demonstrated in their measurement of GGL from the SDSS that the GGL signal is stronger, and extends to much larger separations, for foreground galaxies that are located in regions of high galaxy density. This detection provides a correlation between the GGL signal and the number density of galaxies, and therefore an integral over the 3PCF \mathcal{G} . Furthermore, the galaxy-shear-shear correlation seems to be in the cosmic shear analysis of the COMBO-17 fields by Brown et al. (2003), where they find a stronger-than-average cosmic shear signal in the A901 field, and a weaker-than-average cosmic shear signal in the CDFS, which is a field selected because it is rather poor in brighter galaxies.

The measurement of these galaxy-mass 3PCFs is expected to be considerably easier than measuring the shear 3PCF itself. Note that \mathcal{G} is first order, and G_{\pm} are second order in the shear. For the same reason that GGL measurements are easier to obtain than second-order cosmic shear measurements, the former being just first order in the shear, one therefore expects that \mathcal{G} and G_{\pm} are more straightforward to measure from a given data set. In particular, every wide-field survey in which the shear 3PCF can be measured should yield a significant measurement of these cross-correlation functions.

6. Relation to the bispectrum

It is relatively straightforward to write the correlation functions G_{\pm} and \mathcal{G} in terms of the (projected) bispectra defined in Sect. 4. The complex shear is related to the convergence in Fourier space so that $\hat{\gamma}_c(\boldsymbol{\ell}) = \hat{\kappa}(\boldsymbol{\ell})e^{2i\beta}$, where β is the polar angle of the vector $\boldsymbol{\ell}$. Using this, along with the rule for rotating shears, one can re-write equation (25) as

$$G_+(\boldsymbol{\vartheta}_1, \boldsymbol{\vartheta}_2) = \int \frac{d^2\ell_1}{(2\pi)^2} \int \frac{d^2\ell_2}{(2\pi)^2} e^{-i(\boldsymbol{\ell}_1 \cdot \boldsymbol{\vartheta}_1 + \boldsymbol{\ell}_2 \cdot \boldsymbol{\vartheta}_2)} e^{2i(\beta_1 - \varphi_1)} e^{2i(\beta_2 - \varphi_2)} b_{\kappa\kappa\kappa}(\boldsymbol{\ell}_1, \boldsymbol{\ell}_2; -\boldsymbol{\ell}_1 - \boldsymbol{\ell}_2). \quad (35)$$

Similar relations hold for the correlation functions defined by Eqs. (26) and (31). Next we split the angles φ_i and β_i into their mean and their difference, by writing $\varphi_1 = \zeta - \phi_3/2$, $\varphi_2 = \zeta + \phi_3/2$ and $\beta_1 = \eta' - \psi/2$, $\beta_2 = \eta' + \psi/2$, where ψ represents the angle contained by ℓ_1 and ℓ_2 , and ϕ_3 is the same as in previous sections. Then, we write $\boldsymbol{\ell}_1 \cdot \boldsymbol{\vartheta}_1 + \boldsymbol{\ell}_2 \cdot \boldsymbol{\vartheta}_2 = A \cos(\eta - \nu)$, where $\eta = \eta' - \zeta$, and

$$A^2 = \ell_1^2 \vartheta_1^2 + \ell_2^2 \vartheta_2^2 - 2\ell_1 \ell_2 \vartheta_1 \vartheta_2 \cos(\phi_3 - \psi), \quad e^{2i\nu} = \frac{1}{A^2} \left[2\ell_1 \ell_2 \vartheta_1 \vartheta_2 + (\ell_1 \vartheta_1)^2 e^{i(\phi_3 - \psi)} + (\ell_2 \vartheta_2)^2 e^{-i(\phi_3 - \psi)} \right]. \quad (36)$$

Splitting up the integrals in (35) into polar coordinates in ℓ -space, the η -integral can be performed, yielding

$$G_+(\boldsymbol{\vartheta}_1, \boldsymbol{\vartheta}_2, \phi_3) = \int \frac{d\ell_1 \ell_1}{(2\pi)} \int \frac{d\ell_2 \ell_2}{(2\pi)} \int \frac{d\psi}{(2\pi)} b_{\kappa\kappa\kappa}(\ell_1, \ell_2, \psi) e^{-2i(\phi_3 - \psi)} J_0(A). \quad (37)$$

In a similar manner, we find for G_-

$$G_-(\boldsymbol{\vartheta}_1, \boldsymbol{\vartheta}_2, \phi_3) = \int \frac{d^2\ell_1}{(2\pi)^2} \int \frac{d^2\ell_2}{(2\pi)^2} e^{-i(\boldsymbol{\ell}_1 \cdot \boldsymbol{\vartheta}_1 + \boldsymbol{\ell}_2 \cdot \boldsymbol{\vartheta}_2)} e^{2i(\beta_1 - \varphi_1)} e^{2i(\beta_2 - \varphi_2)} b_{\kappa\kappa\kappa}(\boldsymbol{\ell}_1, \boldsymbol{\ell}_2; -\boldsymbol{\ell}_1 - \boldsymbol{\ell}_2) \quad (38)$$

$$= \int \frac{d\ell_1 \ell_1}{(2\pi)} \int \frac{d\ell_2 \ell_2}{(2\pi)} \int \frac{d\psi}{(2\pi)} b_{\kappa\kappa\kappa}(\ell_1, \ell_2, \psi) e^{4i\nu} J_4(A), \quad (39)$$

and for \mathcal{G}

$$\mathcal{G}(\boldsymbol{\vartheta}_1, \boldsymbol{\vartheta}_2, \phi_3) = \int \frac{d\ell_1 \ell_1}{(2\pi)} \int \frac{d\ell_2 \ell_2}{(2\pi)} \int \frac{d\psi}{(2\pi)} b_{\kappa\kappa\kappa}(\ell_1, \ell_2, \psi) \frac{(\ell_1 e^{-i\psi/2} + \ell_2 e^{i\psi/2})^2}{|\ell|^2} e^{2i\nu} J_2(A), \quad (40)$$

with $|\ell|^2 = \ell_1^2 + \ell_2^2 - 2\ell_1 \ell_2 \cos \psi$. The above results link directly the cross-correlation functions in real space to their equivalent projected bispectra. In a similar fashion, one may also derive a set of inverse relations, i.e expressing the bispectra in terms of Fourier integrals of the correlation functions, beginning with the definition of the bispectrum in Eq. (17). The resulting expressions, which are derived in the same way as above, are

$$b_{\kappa\kappa\kappa}(\boldsymbol{\ell}_1, \boldsymbol{\ell}_2; -\boldsymbol{\ell}_1 - \boldsymbol{\ell}_2) = \int d^2\vartheta_1 \int d^2\vartheta_2 e^{i(\boldsymbol{\ell}_1 \cdot \boldsymbol{\vartheta}_1 + \boldsymbol{\ell}_2 \cdot \boldsymbol{\vartheta}_2)} e^{-2i(\beta_1 - \varphi_1)} e^{-2i(\beta_2 - \varphi_2)} G_-(\boldsymbol{\vartheta}_1, \boldsymbol{\vartheta}_2) \quad (41)$$

$$= \int d^2\vartheta_1 \int d^2\vartheta_2 e^{i(\boldsymbol{\ell}_1 \cdot \boldsymbol{\vartheta}_1 + \boldsymbol{\ell}_2 \cdot \boldsymbol{\vartheta}_2)} e^{-2i(\beta_1 - \varphi_1)} e^{2i(\beta_2 - \varphi_2)} G_+(\boldsymbol{\vartheta}_1, \boldsymbol{\vartheta}_2). \quad (42)$$

$$(43)$$

Using the same transformations of the polar angles as before, one more integration can be carried out, resulting in

$$b_{\kappa\kappa\mathcal{G}}(\ell_1, \ell_2, \psi) = 2\pi \int d\vartheta_1 \vartheta_1 \int d\vartheta_2 \vartheta_2 \int d\phi_3 e^{4i\nu} J_4(A) G_-(\vartheta_1, \vartheta_2, \phi_3) \quad (44)$$

$$= 2\pi \int d\vartheta_1 \vartheta_1 \int d\vartheta_2 \vartheta_2 \int d\phi_3 e^{2i(\psi-\phi_3)} J_0(A) G_+(\vartheta_1, \vartheta_2, \phi_3). \quad (45)$$

In a similar way, we can express the cross-bispectrum $b_{\mathcal{G}\kappa\kappa}$ in terms of \mathcal{G} , yielding

$$b_{\mathcal{G}\kappa\kappa}(\ell_1, \ell_2, \psi) = 2\pi \int d\vartheta_1 \vartheta_1 \int d\vartheta_2 \vartheta_2 \int d\phi_3 \frac{(\ell_1 e^{i\psi/2} + \ell_2 e^{-i\psi/2})^2}{|\ell|^2} e^{-2i\nu} J_2(A) \mathcal{G}(\vartheta_1, \vartheta_2, \phi_3). \quad (46)$$

Using (35) and replacing the cross-bispectrum in favour of G_- , using (41), one can express G_+ in terms of G_- . Similarly, using (39) and (42), we obtain the inverse relation; these read:

$$G_+(\vartheta_1, \vartheta_2, \phi_3) = \frac{2}{\pi} \int d\vartheta \vartheta \int d\phi \frac{[\vartheta e^{i(\phi_3-\phi)/2} - \vartheta_2 e^{-i(\phi_3-\phi)/2}]^4}{[\vartheta^2 + \vartheta_2^2 - 2\vartheta\vartheta_2 \cos(\phi_3 - \phi)]^3} G_-(\vartheta_1, \vartheta, \phi); \quad (47)$$

$$G_-(\vartheta_1, \vartheta_2, \phi_3) = \frac{2}{\pi} \int d\vartheta \vartheta \int d\phi \frac{[\vartheta e^{-i(\phi_3-\phi)/2} - \vartheta_2 e^{i(\phi_3-\phi)/2}]^4}{[\vartheta^2 + \vartheta_2^2 - 2\vartheta\vartheta_2 \cos(\phi_3 - \phi)]^3} G_+(\vartheta_1, \vartheta, \phi). \quad (48)$$

Hence, if the shear field is a pure E-mode field, these interrelations will be satisfied; note that similar equations are valid for the shear 2PCF (Crittenden et al. 2002; Schneider et al. 2002), relating ξ_+ to ξ_- and vice versa.

7. Aperture statistics

In Sect. 5 we defined 3PCFs for the galaxy-mass correlations, and gave practical estimators for measuring them. These 3PCFs were then related to the corresponding bispectra through Fourier transform relations in Sect. 6. As was demonstrated in Schneider et al. (2004), the relation between the shear 3PCF and the underlying projected mass bispectrum is rather complicated and not easy to evaluate. From Eqs. (37) through (40) we observe that the same is true for the relation between the correlation functions considered here and the corresponding bispectra.

However, we can avoid the use of numerically complicated transformations between the 3PCF and the bispectra by considering aperture statistics (Schneider 1996, 1998; van Waerbeke 1998; Crittenden et al. 2002), in the same way as has been done for the shear 3PCF (Jarvis et al. 2004; Schneider et al. 2004) and for the measurement of the second-order bias factor and galaxy-mass correlation coefficient (Hoekstra et al. 2001, 2002). The main reason for this is that the third-order aperture statistics on the one hand provide a very localized measurement of the corresponding bispectra, and on the other hand can be readily evaluated from the corresponding 3PCFs. In this section, we apply the aperture statistics to the galaxy-mass 3PCFs. The aperture mass is defined as

$$M_{\text{ap}}(\theta) = \int d^2\vartheta U_\theta(|\vartheta|) \kappa(\vartheta) = \int d^2\vartheta Q_\theta(|\vartheta|) \gamma_t(\vartheta), \text{ with } Q_\theta(\vartheta) = \frac{2}{\vartheta^2} \int_0^\vartheta d\vartheta' \vartheta' U_\theta(\vartheta') - U_\theta(\vartheta), \quad (49)$$

where U_θ is a weight function of zero total weight, i.e., $\int d\vartheta \vartheta U_\theta(\vartheta) = 0$. The scale of the weight function is described by θ , and γ_t is the tangential shear component as measured with respect to the direction towards the center of the aperture. Furthermore, we define the aperture counts

$$\mathcal{N}(\theta) = \int d^2\vartheta U_\theta(|\vartheta|) \kappa_g(\vartheta) = \frac{1}{N} \int d^2\vartheta U_\theta(|\vartheta|) N(\vartheta), \quad (50)$$

where the final equality follows because U is a compensated filter function. We consider here the filter function introduced by Crittenden et al. (2002), which has also been used by Jarvis et al. (2004) and Schneider et al. (2004). Writing $U_\theta(\vartheta) = \theta^{-2} u(\vartheta/\theta)$, the filter function reads

$$u(x) = \frac{1}{2\pi} \left(1 - \frac{x^2}{2}\right) e^{-x^2/2}; \quad \hat{u}(\eta) = \int d^2x u(|\mathbf{x}|) e^{i\boldsymbol{\eta}\cdot\mathbf{x}} = \frac{\eta^2}{2} e^{-\eta^2/2}; \quad Q_\theta(\vartheta) = \frac{\vartheta^2}{4\pi\theta^4} \exp\left(-\frac{\vartheta^2}{2\theta^2}\right). \quad (51)$$

This choice for U_θ has the disadvantage that the support of the filter is formally infinite; however, the Gaussian factor renders the *effective* range of support finite, since the filter function becomes extremely small for $\vartheta \gtrsim 3\theta$. This disadvantage over other filter functions that have been employed in cosmic shear studies (Schneider et al. 1998) is more than compensated by the convenient mathematical properties, of which we will make extensive use below.

We can now relate the third-order correlations between the aperture measures to the corresponding bispectra. Consider first

$$\langle M_{\text{ap}}(\theta_1)M_{\text{ap}}(\theta_2)\mathcal{N}(\theta_3) \rangle \equiv \langle M_{\text{ap}}M_{\text{ap}}\mathcal{N} \rangle (\theta_1, \theta_2; \theta_3) = \int d^2\vartheta_1 U_{\theta_1}(\boldsymbol{\vartheta}_1) \int d^2\vartheta_2 U_{\theta_2}(\boldsymbol{\vartheta}_2) \int d^2\vartheta_3 U_{\theta_3}(\boldsymbol{\vartheta}_3) \langle \kappa(\boldsymbol{\vartheta}_1)\kappa(\boldsymbol{\vartheta}_2)\kappa_{\text{g}}(\boldsymbol{\vartheta}_3) \rangle .$$

Replacing the κ_i by their Fourier transforms, carrying out the ϑ_i -integrations, making use of (51) and the definition of the bispectra, yields

$$\langle M_{\text{ap}}M_{\text{ap}}\mathcal{N} \rangle (\theta_1, \theta_2; \theta_3) = \int \frac{d^2\ell_1}{(2\pi)^2} \int \frac{d^2\ell_2}{(2\pi)^2} \hat{u}(\ell_1\theta_1) \hat{u}(\ell_2\theta_2) \hat{u}(|\ell_1 + \ell_2|\theta_3) b_{\kappa\kappa_{\text{g}}}(\ell_1, \ell_2; -\ell_1 - \ell_2) . \quad (52)$$

Similarly, we obtain for the galaxy-galaxy-mass aperture correlator

$$\langle \mathcal{N}\mathcal{N}M_{\text{ap}} \rangle (\theta_1, \theta_2; \theta_3) = \int \frac{d^2\ell_1}{(2\pi)^2} \int \frac{d^2\ell_2}{(2\pi)^2} \hat{u}(\ell_1\theta_1) \hat{u}(\ell_2\theta_2) \hat{u}(|\ell_1 + \ell_2|\theta_3) b_{\text{gg}\kappa}(\ell_1, \ell_2; -\ell_1 - \ell_2) . \quad (53)$$

Since \hat{u} is a function that has a very narrow peak, the third-order aperture measures provide very localized information on the respective bispectra and are thus ideal for probing the latter. Unless the bispectra have very sharp features, the third-order aperture measures contain essentially all information about the bispectra – cf. the corresponding discussion for the shear 3PCF and their aperture measures in Schneider et al. (2004). We next show how the third-order aperture measures can be calculated directly in terms of the respective correlation functions. For that, it is convenient to introduce a complex aperture shear measure, defined as

$$M(\theta) := M_{\text{ap}}(\theta) + iM_{\perp}(\theta) = \int d^2\vartheta Q_{\theta}(|\boldsymbol{\vartheta}|) [\gamma_{\text{t}}(\boldsymbol{\vartheta}) + i\gamma_{\times}(\boldsymbol{\vartheta})] = \int d^2\vartheta Q_{\theta}(|\boldsymbol{\vartheta}|) \gamma(\boldsymbol{\vartheta}; \varphi) \quad (54)$$

where φ is the polar angle of $\boldsymbol{\vartheta}$. If the shear field is entirely due to the lensing mass distribution, M_{\perp} vanishes identically (Crittenden et al. 2002). A non-zero value for M_{\perp} would indicate the presence of B-mode shear. In fact $M_{\text{ap}}(\theta)$ vanishes identically for B-modes, whereas $M_{\perp}(\theta)$ yields zero for a pure E-mode field. Thus, the aperture measures are ideally suited to separating E- and B-modes of the shear.

7.1. Galaxy-mass-mass aperture statistics

We will now express the third-order aperture measures to the 3PCFs considered in the previous section. First we find from the definition (54)

$$\langle MMN \rangle (\theta_1, \theta_2; \theta_3) = \int d^2X_1 \int d^2X_2 \int d^2Y Q_{\theta_1}(|\mathbf{X}_1|) Q_{\theta_2}(|\mathbf{X}_2|) U_{\theta_3}(|\mathbf{Y}|) \langle \gamma(\mathbf{X}_1; \psi_1) \gamma(\mathbf{X}_2; \psi_2) \kappa_{\text{g}}(\mathbf{Y}) \rangle , \quad (55)$$

where ψ_i is the polar angle of the vector \mathbf{X}_i , $i = 1, 2$. Next we introduce the separation vectors $\boldsymbol{\vartheta}_i = \mathbf{X}_i - \mathbf{Y}$, and let φ_i denote their polar angle. Then we apply the transformation

$$\gamma(\mathbf{X}_i; \psi_i) = \gamma(\mathbf{Y} + \boldsymbol{\vartheta}_i; \varphi_i) e^{2i(\varphi_i - \psi_i)} = \gamma(\mathbf{Y} + \boldsymbol{\vartheta}_i; \varphi_i) e^{2i\varphi_i} \frac{(\check{Y}^* + \check{\vartheta}_i^*)^2}{|\mathbf{Y} + \boldsymbol{\vartheta}_i|^2} , \quad (56)$$

where we have introduced the notation that a two-dimensional vector \mathbf{X} can be written as a complex number $\check{X} := X_1 + iX_2$, which is convenient for expressing phases: If φ is the polar angle of \mathbf{X} , then $e^{i\varphi} = \check{X}/|\mathbf{X}|$. Inserting the foregoing expression into (55) and using the definition (51) of the filter functions, one obtains

$$\begin{aligned} \langle MMN \rangle (\theta_1, \theta_2; \theta_3) &= \frac{1}{(4\pi)^3 \theta_1^4 \theta_2^4 \theta_3^4} \int d^2\vartheta_1 e^{2i\varphi_1} \int d^2\vartheta_2 e^{2i\varphi_2} G_{-}(\boldsymbol{\vartheta}_1, \boldsymbol{\vartheta}_2) \\ &\quad \times \int d^2Y \left(\check{Y}^* + \check{\vartheta}_1^* \right)^2 \left(\check{Y}^* + \check{\vartheta}_2^* \right)^2 (2\theta_3^2 - |\mathbf{Y}|^2) \exp \left[- \left(\frac{|\mathbf{Y} + \boldsymbol{\vartheta}_1|^2}{2\theta_1^2} + \frac{|\mathbf{Y} + \boldsymbol{\vartheta}_2|^2}{2\theta_2^2} + \frac{|\mathbf{Y}|^2}{2\theta_3^2} \right) \right] . \end{aligned} \quad (57)$$

The \mathbf{Y} -integration can be performed, and the result, when multiplied with the phase factors, only depends on the modulus of the $\boldsymbol{\vartheta}_i$ and the angle ϕ_3 they enclose. Hence,

$$\langle MMN \rangle (\theta_1, \theta_2; \theta_3) = \int_0^{\infty} d\vartheta_1 \vartheta_1 \int_0^{\infty} d\vartheta_2 \vartheta_2 \int_0^{2\pi} d\phi_3 G_{-}(\vartheta_1, \vartheta_2, \phi_3) A_{MMN}(\vartheta_1, \vartheta_2, \phi_3 | \theta_1, \theta_2; \theta_3) , \quad (58)$$

where the convolution function $A_{MM\mathcal{N}}$ is given in the appendix. In the same way, we can evaluate

$$\begin{aligned} \langle MM^*\mathcal{N} \rangle (\theta_1, \theta_2; \theta_3) &= \frac{1}{(4\pi)^3 \theta_1^4 \theta_2^4 \theta_3^4} \int d^2\vartheta_1 e^{2i\varphi_1} \int d^2\vartheta_2 e^{-2i\varphi_2} G_+(\boldsymbol{\vartheta}_1, \boldsymbol{\vartheta}_2) \\ &\times \int d^2Y \left(\check{Y}^* + \check{\vartheta}_1^* \right)^2 \left(\check{Y} + \check{\vartheta}_2 \right)^2 (2\theta_3^2 - |\mathbf{Y}|^2) \exp \left[- \left(\frac{|\mathbf{Y} + \boldsymbol{\vartheta}_1|^2}{2\theta_1^2} + \frac{|\mathbf{Y} + \boldsymbol{\vartheta}_2|^2}{2\theta_2^2} + \frac{|\mathbf{Y}|^2}{2\theta_3^2} \right) \right] \end{aligned} \quad (59)$$

$$= \int_0^\infty d\vartheta_1 \vartheta_1 \int_0^\infty d\vartheta_2 \vartheta_2 \int_0^{2\pi} d\phi_3 G_+(\vartheta_1, \vartheta_2, \phi_3) A_{MM^*\mathcal{N}}(\vartheta_1, \vartheta_2, \phi_3 | \theta_1, \theta_2; \theta_3), \quad (60)$$

where again the convolution function is given in the appendix. By combining (58) and (59), one finds

$$\begin{aligned} \langle M_{\text{ap}} M_{\text{ap}} \mathcal{N} \rangle (\theta_1, \theta_2; \theta_3) &= \Re [\langle MM\mathcal{N} \rangle (\theta_1, \theta_2; \theta_3) + \langle MM^*\mathcal{N} \rangle (\theta_1, \theta_2; \theta_3)] / 2 \\ \langle M_\perp M_\perp \mathcal{N} \rangle (\theta_1, \theta_2; \theta_3) &= \Re [\langle MM^*\mathcal{N} \rangle (\theta_1, \theta_2; \theta_3) - \langle MM\mathcal{N} \rangle (\theta_1, \theta_2; \theta_3)] / 2 \\ \langle M_\perp M_{\text{ap}} \mathcal{N} \rangle (\theta_1, \theta_2; \theta_3) &= \Im [\langle MM\mathcal{N} \rangle (\theta_1, \theta_2; \theta_3) + \langle MM^*\mathcal{N} \rangle (\theta_1, \theta_2; \theta_3)] / 2. \end{aligned}$$

The first of these is the expression that is directly related to the bispectrum $b_{\kappa\kappa\text{g}}$. The second expression is expected to vanish if the shear is caused solely by gravitational lensing. A significant non-zero value of this correlator would indicate the presence of B-mode shear which is correlated with the foreground galaxy distribution. The final expression is expected to be zero because it is not parity-invariant, as all odd-order statistics in B-mode shear (Schneider 2003); hence, a measured non-zero value would indicate that the data violate parity invariance.

One may consider how the results defined above would change if the modified correlators \tilde{G}_\pm were used in the definition of $\langle MM^*\mathcal{N} \rangle$ and $\langle MM\mathcal{N} \rangle$. Using the fact that $N/\tilde{N} = \kappa_{\text{g}} + 1$ we find, using Eq. (55), that since U is a compensated filter, the additional terms arising from two point shear-shear correlations vanish. Thus we make the following useful assertion that when working with the aperture mass statistics, one need not subtract the contribution from the shear 2PCF to compute the reduced three point statistics.

7.2. Galaxy-galaxy-mass aperture statistics

Finally, we consider the galaxy-galaxy-mass third-order aperture statistics

$$\langle \mathcal{N}\mathcal{N}M \rangle (\theta_1, \theta_2; \theta_3) = \int d^2X_1 \int d^2X_2 \int d^2Y U_{\theta_1}(|\mathbf{X}_1|) U_{\theta_2}(|\mathbf{X}_2|) Q_{\theta_3}(|\mathbf{Y}|) \langle \kappa_{\text{g}}(\mathbf{X}_1) \kappa_{\text{g}}(\mathbf{X}_2) \gamma(\mathbf{Y}; \psi) \rangle, \quad (61)$$

where ψ is the polar angle of \mathbf{Y} . Again introducing the separation vectors $\boldsymbol{\vartheta}_i = \mathbf{X}_i - \mathbf{Y}$, which have polar angles φ_i , $i = 1, 2$, using the transformation

$$\gamma(\mathbf{Y}; \psi) = \gamma \left(\mathbf{Y}; \frac{\varphi_1 + \varphi_2}{2} \right) e^{i(\varphi_1 + \varphi_2 - 2\psi)} = \gamma \left(\mathbf{Y}; \frac{\varphi_1 + \varphi_2}{2} \right) e^{i\varphi_1} e^{i\varphi_2} \frac{(\check{Y}^*)^2}{|\mathbf{Y}|^2}, \quad (62)$$

and inserting the definitions (51) into (61) yields

$$\begin{aligned} \langle \mathcal{N}\mathcal{N}M \rangle (\theta_1, \theta_2; \theta_3) &= \frac{1}{(4\pi)^3 \theta_1^4 \theta_2^4 \theta_3^4} \int d^2\vartheta_1 e^{i\varphi_1} \int d^2\vartheta_2 e^{i\varphi_2} \mathcal{G}(\boldsymbol{\vartheta}_1, \boldsymbol{\vartheta}_2) \\ &\times \int d^2Y (2\theta_1^2 - |\mathbf{Y} + \boldsymbol{\vartheta}_1|^2) (2\theta_2^2 - |\mathbf{Y} + \boldsymbol{\vartheta}_2|^2) (\check{Y}^*)^2 \exp \left[- \left(\frac{|\mathbf{Y} + \boldsymbol{\vartheta}_1|^2}{2\theta_1^2} + \frac{|\mathbf{Y} + \boldsymbol{\vartheta}_2|^2}{2\theta_2^2} + \frac{|\mathbf{Y}|^2}{2\theta_3^2} \right) \right] \end{aligned} \quad (63)$$

$$= \int_0^\infty d\vartheta_1 \vartheta_1 \int_0^\infty d\vartheta_2 \vartheta_2 \int_0^{2\pi} d\phi_3 \mathcal{G}(\vartheta_1, \vartheta_2, \phi_3) A_{\mathcal{N}\mathcal{N}M}(\vartheta_1, \vartheta_2, \phi_3 | \theta_1, \theta_2; \theta_3), \quad (64)$$

where the convolution function is also derived in the appendix. The real part of $\langle \mathcal{N}\mathcal{N}M \rangle$ corresponds to the aperture 3PCF that is directly related to the bispectrum $b_{\text{gg}\kappa}$, whereas the imaginary part vanishes due to parity invariance. Finally in this section we note that, as with the galaxy-mass-mass statistics, the quantity $\langle \mathcal{N}\mathcal{N}M \rangle$ does not change when the definition for $\tilde{\mathcal{G}}$ is used in place of \mathcal{G} in Eq. (61). Second-order galaxy-galaxy lensing effects are therefore not important for the three-point aperture mass statistics.

8. Discussion

In this paper, we have defined third-order galaxy-mass correlation functions and the corresponding third-order bias factor and related them to quantities which can be measured directly through galaxy-galaxy-galaxy lensing. Whereas the underlying physical quantities are the bispectra of the mass and galaxy distribution, as well as the cross-bispectra, the observables are the shear as measured from the ellipticity of background galaxies in relation to the position of

foreground galaxies. We have argued that these third-order correlations have probably been measured already, and are almost certainly measurable from data sets existing now; the ongoing and planned wide-field surveys will obtain precision measurements of these third-order statistics. The basic observables are the 3PCFs, as their measurement is not affected by holes and gaps in the data set which are unavoidable due to the selection of the survey geometry and masking of bright stars and galaxies, as well as CCD defects. The 3PCFs are related to the corresponding bispectra through a very broad and oscillating filter function (see Schneider et al. 2004 for the case of the shear 3PCF) and thus do not directly provide information about the shape of the bispectra. Therefore, we have considered the aperture statistics, which on the one hand can be calculated readily from the measured correlation functions, and on the other hand are related to the bispectra through a narrow filter function, hence providing localized information on the latter. In fact, unless the bispectra vary strongly as a function of their angular wave vectors ℓ_i , the third-order aperture measures are expected to contain essentially all information about the third-order galaxy-mass correlations. Furthermore, the aperture measures allow one to easily identify the presence of B-modes in the shear field, as well as unphysical parity-violating contributions, which can only be due to the observing and data reduction steps, unless we drop the assumption that the mass distribution in our Universe is parity invariant.

The convolution functions relating the 3PCFs to the third-order aperture measures have in principle an infinite support; in practice, however, the exponential factor implies that the 3PCFs have to be measured only up to a few times the corresponding filter scales θ_i . Therefore, these convolution functions have essentially finite support.

Nevertheless, in order to calculate the third-order aperture measures, the corresponding correlation functions need to be measured to $\sim 6\theta_{\max}$, where θ_{\max} is the largest of the three aperture radii. The largest scale on which the correlation functions can be measured is determined by the geometry of the survey. For a large survey with contiguous area, this scale is limited by the smallness of the signal when entering the linear regime of structure evolution. In this case, the aperture measures contain all the information contained in the measured correlation functions. If the survey consists of independent patches each of size ψ , then the correlation functions can be measured for angular scales up to $\sim \psi$, meaning that the aperture measures are limited to $\theta_{\max} \lesssim \psi/6$. In this case, the measured correlation functions contain more information than the aperture measures. In a future work, we plan to study these aspects; note, however, that estimates of the ‘information content’ are tedious, since they involve the covariance of third-order statistical measures, and thus depend, in general, on six variables and have to be estimated from sixth-order statistics.

The correlation function \mathcal{G} measures the same cross-bispectrum as the third-order statistics considered by Ménard et al. (2003). In that paper, they considered the correlation between pairs of foreground galaxies and background QSOs. Due to the magnification of distant QSOs by the matter in which the foreground galaxies are embedded, and the steep slope of bright QSO source counts, such a correlation should be measurable with the large QSO sample obtained by the Sloan Digital Sky Survey. Instead of magnification, we employ the shear around galaxy pairs. Which of the two methods is better able to measure the galaxy-mass bispectrum depends on the available observational data. For deep wide-field images, the shear method investigated here will be more efficient, given the sparseness of bright QSOs on the sky.

As is true for the second-order galaxy-mass correlations, as measured in GGL, the physical interpretation of the third-order correlations is not straightforward, but needs to be done in the frame of a model. On very large scales, we might expect that b_3 essentially becomes a constant, but that will be difficult to measure, as on these large scales, the density field is expected to quickly approach a Gaussian, and thus the bispectrum should be very small.

A useful analytic description of clustering statistics on all cosmological scales is given by the halo model (see Cooray & Sheth 2002 for a review). Within this framework it will be possible to relate the higher-order cross-correlation functions to the quantities that specify the Halo Occupation Distribution. As pointed out by Berlind & Weinberg (2002) the HOD essentially contains *all* of the information about the statistics of galaxy clustering that theories of galaxy formation are able to provide; it is a complete description of the bias. Future empirical determinations of the HOD using observations of galaxy and mass clustering will enable powerful constraints to be placed on the development of models for galaxy formation. In a forthcoming paper we shall explore these concepts in detail, building the physical interpretation of our third-order galaxy-mass correlations using the halo model and the HOD.

Acknowledgements. We thank Martin Kilbinger for useful comments on the manuscript. This work was supported by the German Ministry for Science and Education (BMBF) through the DLR under the project 50 OR 0106 and by the Deutsche Forschungsgemeinschaft under the project SCHN 342/3-1.

Appendix A: The convolution functions

In this appendix, we derive the convolution functions which relate the third-order aperture measures to the corresponding 3PCFs. We start by rewriting the exponent in (57), (59) and (63) by making a translation $\mathbf{Y} = \mathbf{y} - \mathbf{c}$, where \mathbf{c} is chosen so as to remove linear terms in \mathbf{y} ,

$$\frac{|\mathbf{Y} + \boldsymbol{\vartheta}_1|^2}{2\theta_1^2} + \frac{|\mathbf{Y} + \boldsymbol{\vartheta}_2|^2}{2\theta_2^2} + \frac{|\mathbf{Y}|^2}{2\theta_3^2} = \frac{|\mathbf{y}|^2}{a_2} + b_0; \quad a_2 = \frac{2\theta_1^2\theta_2^2\theta_3^2}{\theta_1^2\theta_2^2 + \theta_1^2\theta_3^2 + \theta_2^2\theta_3^2}; \quad \mathbf{c} = \frac{a_2}{2} \left(\frac{\boldsymbol{\vartheta}_1}{\theta_1^2} + \frac{\boldsymbol{\vartheta}_2}{\theta_2^2} \right); \quad (\text{A.1})$$

$$b_0 = \frac{|\boldsymbol{\vartheta}_1|^2}{2\theta_1^2} + \frac{|\boldsymbol{\vartheta}_2|^2}{2\theta_2^2} - \frac{|\mathbf{c}|^2}{a_2} = \frac{\vartheta_1^2}{2\theta_1^2} + \frac{\vartheta_2^2}{2\theta_2^2} - \frac{a_2}{4} \left(\frac{\vartheta_1^2}{\theta_1^4} + \frac{2\vartheta_1\vartheta_2 \cos \phi_3}{\theta_1^2\theta_2^2} + \frac{\vartheta_2^2}{\theta_2^4} \right). \quad (\text{A.2})$$

Next, we consider the prefactor of the exponential in (57), and change the integration variable from \mathbf{Y} to \mathbf{y} . For this, we first define

$$\left(\check{Y}^* + \check{y}_i^* \right) e^{i\varphi_i} = \check{y}^* e^{i\varphi_i} + \vartheta_i - \check{c}^* e^{i\varphi_i} \equiv \check{y}^* e^{i\varphi_i} + \check{g}_i, \quad \vartheta_i \equiv |\boldsymbol{\vartheta}_i|, \quad (\text{A.3})$$

for $i = 1, 2$, or more explicitly,

$$\check{g}_1 = \vartheta_1 - \frac{a_2}{2} \left(\frac{\vartheta_1}{\theta_1^2} + \frac{\vartheta_2 e^{-i\phi_3}}{\theta_2^2} \right); \quad \check{g}_2 = \vartheta_2 - \frac{a_2}{2} \left(\frac{\vartheta_2}{\theta_2^2} + \frac{\vartheta_1 e^{i\phi_3}}{\theta_1^2} \right). \quad (\text{A.4})$$

The prefactor of the exponential, when multiplied with the phase factors, then becomes

$$\begin{aligned} F'_{MMN} &= (\check{y}^* e^{i\varphi_1} + \check{g}_1)^2 (\check{y}^* e^{i\varphi_2} + \check{g}_2)^2 (2\theta_3^2 - |\mathbf{y}|^2 - |\mathbf{c}|^2 + \check{c}\check{y}^* + \check{c}^*\check{y}) \\ &= \check{g}_1^2\check{g}_2^2 (2\theta_3^2 - |\mathbf{y}|^2 - |\mathbf{c}|^2) + 2|\mathbf{y}|^2\check{g}_1\check{g}_2 [\check{g}_2(\vartheta_1 - \check{g}_1) + \check{g}_1(\vartheta_2 - \check{g}_2)] + C = F_{MMN} + C, \end{aligned} \quad (\text{A.5})$$

where C denotes additional terms which, however, become zero when the \mathbf{y} -integration is carried out, since the exponent depends only on $|\mathbf{y}|^2$. The \mathbf{y} -integration can now be carried out,

$$\int d^2y F'_{MMN} e^{-|\mathbf{y}|^2/a_2} = 2\pi \int_0^\infty dy y F_{MMN} e^{-|\mathbf{y}|^2/a_2} = \pi a_2^2 \check{g}_1 \check{g}_2 \left[\left(\frac{\theta_3^2}{\theta_1^2} + \frac{\theta_3^2}{\theta_2^2} - \frac{|\mathbf{c}|^2}{a_2} \right) \check{g}_1 \check{g}_2 + 2(\check{g}_2 \vartheta_1 + \check{g}_1 \vartheta_2 - 2\check{g}_1 \check{g}_2) \right].$$

The result depends only on ϑ_1, ϑ_2 and the angle ϕ_3 between $\boldsymbol{\vartheta}_1$ and $\boldsymbol{\vartheta}_2$, so that an additional angular integration can be carried out in Eq. (57). We thus arrive at (58), with

$$A_{MMN} = \frac{\check{g}_1 \check{g}_2 e^{-b_0}}{72\pi\Theta^8} \left[\left(\frac{\theta_3^2}{\theta_1^2} + \frac{\theta_3^2}{\theta_2^2} - \frac{|\mathbf{c}|^2}{a_2} \right) \check{g}_1 \check{g}_2 + 2(\check{g}_2 \vartheta_1 + \check{g}_1 \vartheta_2 - 2\check{g}_1 \check{g}_2) \right]; \quad \Theta^4 = \frac{\theta_1^2\theta_2^2 + \theta_1^2\theta_3^2 + \theta_2^2\theta_3^2}{3}. \quad (\text{A.6})$$

Similar expansions of the prefactors of the exponentials in Eqs. (59) and (63) can also be determined using the same definitions as above. Performing the relevant integrals, we find that the convolution factors for equations (60) and (64) are then given by

$$\begin{aligned} A_{MM^*\mathcal{N}} &= \frac{e^{-b_0}}{72\pi\Theta^8} \left[2(\vartheta_1 \check{g}_2^* + \vartheta_2 \check{g}_1 - 2\check{g}_1 \check{g}_2^*) (\check{g}_1 \check{g}_2^* + 2a_2 e^{-i\phi_3}) + 2a_2 (2\theta_3^2 - |\mathbf{c}|^2 - 3a_2) e^{-2i\phi_3} \right. \\ &\quad \left. + 4\check{g}_1 \check{g}_2^* (2\theta_3^2 - |\mathbf{c}|^2 - 2a_2) e^{-i\phi_3} + \frac{(\check{g}_1 \check{g}_2^*)^2}{a_2} (2\theta_3^2 - |\mathbf{c}|^2 - a_2) \right] \end{aligned} \quad (\text{A.7})$$

and

$$\begin{aligned} A_{\mathcal{N}\mathcal{N}M} &= \frac{e^{-b_0}}{72\pi\Theta^8} \left\{ (\check{g}_1 - \vartheta_1) (\check{g}_2 - \vartheta_2) \left[\frac{1}{a_2} F_1 F_2 - (F_1 + F_2) + 2a_2 + \check{g}_1^* \check{g}_2 e^{-i\phi_3} + \check{g}_1 \check{g}_2^* e^{i\phi_3} \right] \right. \\ &\quad \left. - [(\check{g}_2 - \vartheta_2) + (\check{g}_1 - \vartheta_1) e^{i\phi_3}] [\check{g}_1 (F_2 - 2a_2) + \check{g}_2 (F_1 - 2a_2) e^{-i\phi_3}] + 2\check{g}_1 \check{g}_2 a_2 \right\} \end{aligned} \quad (\text{A.8})$$

where $F_i = 2\theta_i^2 - |\check{g}_i|^2$.

References

- Bacon, D.J., Refregier, A.R. & Ellis, R.S. 2000, MNRAS, 318, 625
 Bartelmann M., Schneider P., 2001, Phys. Rep., 340, 291 (BS01)
 Berlind A. & Weinberg, D. 2002, ApJ 575, 587
 Bernardeau, F., Mellier, Y. & van Waerbeke, L. 2002, A&A 389, L28
 Bernardeau, F., van Waerbeke, L. & Mellier, Y. 1997, A&A, 322, 1

- Blandford, R.D., Saust, A.B., Brainerd, T.G. & Villumsen, J.V. 1991, MNRAS, 251, 600
- Brainerd, T.G., Blandford, R.D., & Smail, I. 1996, ApJ, 466, 623
- Brown, M.L., Taylor, A.N., Bacon, D.J. et al. 2003, MNRAS 341, 100
- Cooray, A. & Sheth, R. 2002, PhR 372, 1
- Crittenden, R.G., Natarajan, P., Pen, U.-L. & Theuns, T. 2002, ApJ, 568, 20
- Croft, R.A.C. & Metzler, C.A. 2001, ApJ, 545, 561
- Dell'Antonio, I.P. & Tyson, J.A. 1996, ApJ 473, L17
- Dolag, K. & Bartelmann, M. 1997, MNRAS 291, 446
- Fischer, P., McKay, T.A., Sheldon, E. et al. 2000, AJ 120, 1198
- Griffiths, R.E., Casertano, S., Im, M. & Ratnatunga, K.U. 1996, MNRAS 282, 1159
- Guzik, J. & Seljak, U. 2002, MNRAS 335, 311
- Hoekstra, H., van Waerbeke, L., Gladders, M.D., Mellier, Y. & Yee, H.K.C. 2002, ApJ 577, 604
- Hoekstra, H., Yee, H.K.C. & Gladders, M.D. 2001, ApJ 558, L11
- Hudson, M.J., Gwyn, S.D.J., Dahle, H. & Kaiser, N. 1998, ApJ 503, 531
- Jain, B. & Seljak, U. 1997, ApJ, 484, 560
- Jarvis, M., Bernstein, G.M., Fischer, P. et al. 2003, AJ 125, 1014
- Jarvis, M., Bernstein, G.M. & Jain, B. 2004, MNRAS 352, 338
- Kaiser, N. 1992, ApJ, 388, 272
- Kaiser, N., Wilson, G. & Luppino, G. 2000, astro-ph/0003338
- Kleinheinrich, M., Rix, H.-W., Erben, T., et al. 2004, A&A submitted (also astro-ph/0404527)
- Maoli, R., van Waerbeke, L., Mellier, Y. et al. 2001, A&A 368, 766
- McKay, T.A., Sheldon, E.S., Racusin, J. et al. 2001, astro-ph/0108013
- Mellier, Y. 1999, ARA&A, 37, 127
- Ménard, B., Bartelmann, M. & Mellier, Y. 2003, A&A 409, 411
- Miralda-Escudé, J. 1991, ApJ 380, 1
- Peebles, P.J.E. 1980, *The large-scale structure of the universe*, Princeton University Press
- Pen, U.-L., Zhang, T., van Waerbeke, L., Mellier, Y., Zhang, P. & Dubinski, J. 2003, ApJ 592, 664
- Refregier, A. 2003, ARA&A 41, 645
- Refregier, A. Rhodes, J. & Groth, E.J. 2002, ApJ 572, L131
- Schneider, P. 1996, MNRAS, 283, 837
- Schneider, P. 1998, ApJ 498, 43
- Schneider, P. 2003, A&A 408, 829
- Schneider, P., Kilbinger, M. & Lombardi, M. 2004, A&A, submitted (also astro-ph/0308328)
- Schneider, P. & Lombardi, M. 2003, A&A 397, 809
- Schneider, P., van Waerbeke, L. & Mellier, Y. 2002, A&A 389, 729
- Schneider, P., van Waerbeke, L., Jain, B., Kruse, G., 1998, MNRAS, 296, 873
- Seljak, U., Makarov, A., Mandelbaum, R. et al. 2004, astro-ph/0406594
- Sheldon, E.S., Johnston, D.E., Frieman, J.A. et al. 2004, AJ 127, 2544
- Takada, M. & Jain, B. 2003a, ApJ 583, L49
- Takada, M. & Jain, B. 2003b, MNRAS 344, 857
- Tyson, J.A., Valdes, F., Jarvis, J.F. & Mills Jr., A.P. 1984, ApJ 281, L59
- Van Waerbeke, L. 1998, A&A 334, 1
- van Waerbeke, L., Bernardeau, F. & Mellier, Y. 1999, A&A, 243, 15
- Van Waerbeke, L., Mellier, Y., Erben, T. et al. 2000, A&A, 358, 30
- Van Waerbeke, L., Mellier, Y., Radovich, M. et al. 2001, A&A, 374, 757
- van Waerbeke, L. & Mellier, Y. 2003, astro-ph/0305089
- van Waerbeke, L., Mellier, Y., Pello, R., et al. 2002, A&A 393, 369
- Wittman, D.M., Tyson, J.A., Kirkman, D., Dell'Antonio, I. & Bernstein, G. 2000, Nat, 405, 143
- Zaldarriaga, M. & Scoccimarro, R. 2003, ApJ 584, 559